A 6–21-GHz Monolithic HEMT 2 × 3 Matrix Distributed Amplifier

K. W. Kobayashi, R. Esfandiari, *Member, IEEE*, W. L. Jones, *Member, IEEE*, K. Minot, B. R. Allen, *Member, IEEE*, A. Freudenthal, and D. C. Streit, *Member, IEEE*

***Abstract*—The results of the first monolithic matrix distributed amplifier fabricated using pseudomorphic HEMT technology are reported. The HEMT matrix amplifier obtains a combination of high gain, wide bandwidth, and reasonable IP3 and noise figure. The best gain response is 20 dB from 6–21 GHz. The noise figure is 5.5 dB and the third-order intercept point is 21 dBm. In comparison to GaAs HBT and MESFET technologies, the HEMT matrix distributed amplifier shows the best promise for wide-band millimeter-wave applications.**

I. Introduction

Matrix distributed amplifiers are noted for their high gain and bandwidth and compact layout characteristics. The monolithic matrix distributed amplifier was introduced using MESFET technology and several papers on measured results and theory have been reported by these authors [1], [2]. Matrix distributed amplifiers have also been implemented with (HBT) heterojunction bipolar transistor technology [3], [4]. Both MESFET and HBT technologies have exhibited high-gain bandwidth responses. To a first order, the gain-bandwidth product is proportional to the ratio of the device G_m to $C_{gs}(C_\pi)$ for distributed amplifier type designs. This neglects the attenuation along the transmission lines due to device parasitic resistances. Table I gives typical device hybrid-π model parameters for the different technologies at a given bias current. A 0.25-μm GaAs MESFET, a 2-μm self-aligned base ohmic metal HBT, and a 0.2-μm pseudomorphic HEMT technology is compared. Parameter $G_{m\text{eff}}$, incorporates the emitter or source resistance which degrades the device's inherent G_m. For a given current, HBT's have the highest intrinsic transconductance, G_m, which is 4–5 times greater than HEMT's and an order of magnitude higher than MESFET's. When comparing $G_{m\text{eff}}$ however, the differences are not as great, but are still significant. The input capacitances C_{gs} and C_π show that HBT's have an order of magnitude higher input capacitance than either the HEMT's or MESFET's. This is due to the diffusion capacitance of the forward biased base-emitter junction of the HBT. Table I shows that the $G_{m\text{eff}}/C_{gs}$ ratio is higher for HEMT's than for MESFET's or HBT's and therefore, can achieve higher gain-bandwidth products in distributed amplifier designs. In reality, the parasitic resistances limit the amount of device periphery that can be added to increase the gain-bandwidth product. When we compare the parasitic resistances of the different technologies, we find that r_s, r_g, r_e, and r_b are small and can be reduced with improved technology. Thus, from our simplistic comparison, HEMT technology is the best choice for achieving wide gain-bandwidths with the matrix topology. The following sections report on the design, fabrication, and measurement results of a matrix amplifier implemented with HEMT's.

Manuscript received September 28, 1992.

The authors are with TRW, Electronic and Technology Division, One Space Park, Redondo Beach, CA 90278.

IEEE Log Number 9206158.

II. HEMT Amplifier Process

The pseudomorphic InGaAs HEMT is used to fabricate the amplifier because of its high gain and power capacity. The active layers are grown by MBE, and oxygen implantation is used for a planar isolation. Ohmic contacts consisting of Ni–AuGe–Ag–Au are alloyed using rapid thermal anneal. A low-contact resistance is essential for a high-performance device. Using this process, contact resistances of less than 0.15 Ω-mm^2 can be achieved. Nichrome thin-film resistors are evaporated and lifted off before the EBL gate process. The baseline 0.2-μm T-gate is delineated by E-beam lithography. Ti–Pt–Au is used for low-resistance interconnects. MIM capacitors are formed using low-temperature SiO_2. Airbridge and top metal consisting of 2.0-μm gold are used for crossover interconnects and microstrip transmission lines. After completion of the frontside process, the wafers are thinned to 4 mils, and vias are etched through the wafer for low-inductance grounding. The two key steps of the HEMT fabrication process are submicron E-beam lithography and MBE growth. Exellent reproducibility has been demonstrated for the gate process with control of better than ±0.03 μm. The MBE-grown PM InGaAs HEMT wafers have consistently shown room temperature mobilities in excess of 4500 cm^2/V-s.

III. Amplifier Design

The HEMT 2 × 3 matrix amplifier schematic is shown in Fig. 1. The devices used in the input row are 0.2-μm length by 150-μm gate width (Q11, Q12, Q13). The output row has 200 μm gate widths (Q21, Q22, Q23). These devices have excellent frequency characteristics with f_t's of 60 GHz. The input transmission-line cut-off frequency is determined by the C_{gs} of the HEMT's of the input row of the matrix. The output row HEMT's can be chosen to be a larger size since the output cut-off frequency is limited by the size of C_{ds}, which is much smaller than C_{gs}. Also, C_{dg} limits the size of the output devices since it influences the upper band edge stability. Too

TABLE I
COMPARING MESFET, HBT, AND HEMT HYBRID-π MODEL PARAMETERS ($I \approx 16$ MA)

Technology	Size	I_{ds} (mA)	G_m (mS)	$C_{gs}[C_\pi]$ (pF)	$R_g[R_b](\Omega)$	$R_s[R_e](\Omega)$	G_{meff} (mS)	G_{meff}/C_{gs} (GHz)
MESFET	0.25×150 μm	19	35	0.13	4.2	0.38	34.5	266
HBT	2×40 μm	16	615	2.4	7	4	178	74
HEMT	0.2×200 μm	16	100	0.2	2	0.2	98	490

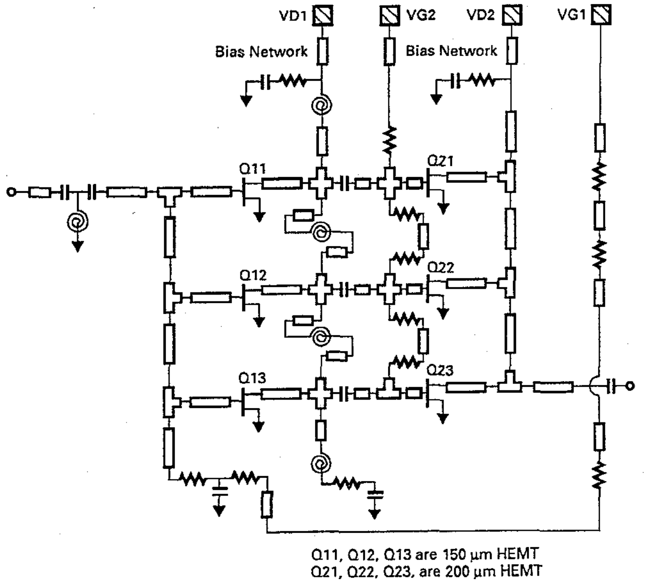

Fig. 1. Schematic of the 6-21 GHz HEMT 2 x 3 matrix distributed amplifier.

large a Cdg causes instability. This is illustrated by the gain peaking at the upper end. The interstage transmission lines can be sythesized to an impedance other than 50 ohms, thus giving freedom to choose a larger output transistor with larger C_{gs}. A high-pass filter was designed to obtain a 6–21-GHz band-pass response. The amplifier was then tuned for optimal gain-bandwidth response. The fabricated amplifier is shown in Fig. 2.

Typical gain and return-loss responses are shown in Fig. 3. The nominal gain for a typical response is 15 dB. The bias condition is $V_{ds1} = 2$ V, $V_{ds2} = 2$ V, $I_{ds1} = 83$ mA, and $I_{ds2} = 123$ mA. The return-loss was about 10 dB or better over the band. At the upper band edge (20 GHz), there is a resonance in the return-losses and a slight peaking in the gain response. This is believed to be caused by C_{dg} as previously mentioned. A measurement at higher bias currents ($V_{ds1} = V_{ds2} = 2.85$ V, $I_{ds1} = 130$ mA, $I_{ds2} = 150$ mA, on a different wafer) gave a nominal gain of 20 dB up to 21 GHz. The 3-dB gain bandwidth product (GBP) is 210 GHz and is the highest reported for a matrix amplifier in any technology. The GBP was calculated assuming a dc to 3-dB frequency bandwidth. Fig. 4 shows the noise figure at a bias of $V_{ds1} =$ 2.5 V, $V_{ds2} = 2.5$ V, $I_{ds1} = 100$ mA, and $I_{ds2} = 100$ mA. The noise is around 5–5.5 dB. However, design simulations show that this amplifier when biased at the minimum noise bias, should be able to achieve as low as 3-dB minimum noise figure (the illustrated design is optimized for gain-bandwidth product). At the nominal gain bias (15 dB), the IP3 averaged 21 dBm across the band.

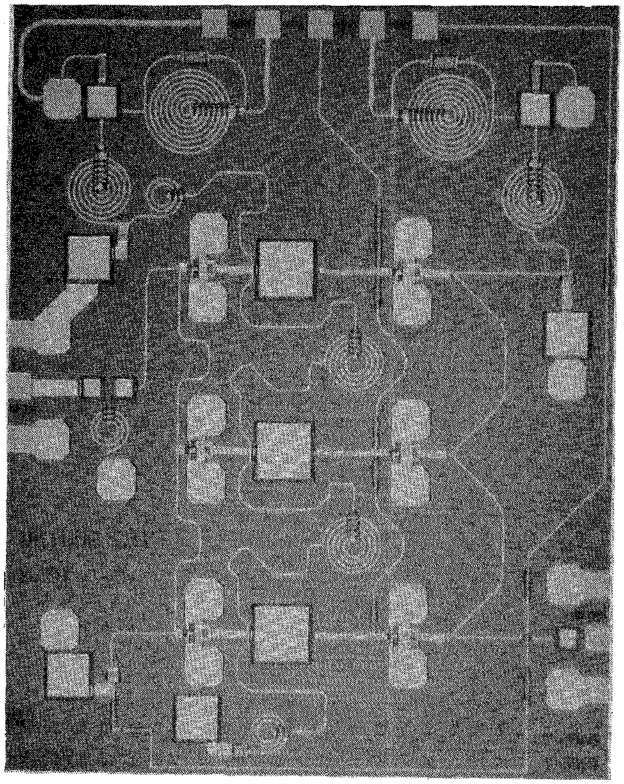

Fig. 2. Photograph of the MMIC HEMT 2 × 3 matrix distributed amplifier. Chip size is 2.6 × 2.5 mm^2.

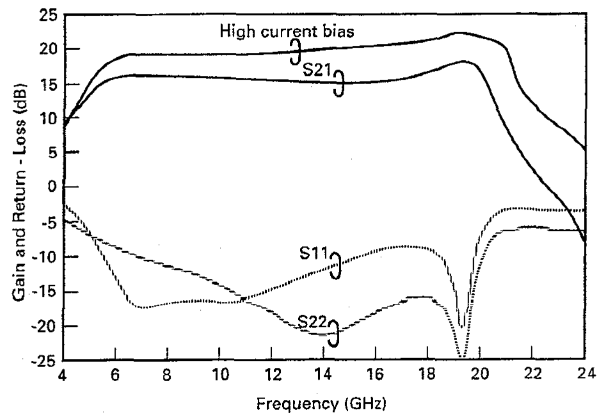

Fig. 3. Typical gain and return-loss performance.

IV. CONCLUSION

Design, fabrication, and measured results of a 6–21-GHz pseudomorphic InGaAs HEMT monolithic matrix distributed

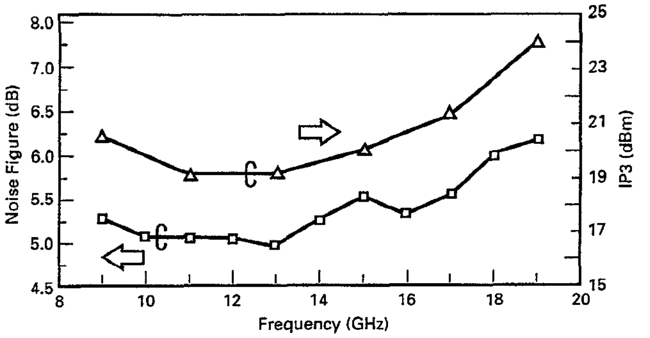

Fig. 4. Typical noise figure and IP3 performance.

amplifier are presented. The measured results indicate that HEMT technology is best suited for high-gain bandwidth performance because of its inherent physical properties that lead to a higher G_m to C_{gs} ratio. This amplifier achieved 20-dB gain and 5.5-dB noise figure over the 6–21-GHz bandwidth. This HEMT matrix distributed amplifier benchmarks the highest gain bandwidth product reported for any GaAs technology.

Acknowledgment

The authors would like to acknowledge the support of J. B. Horton who supplied IR&D funding for this design. Also, we would like to recognize P. Rogers, K. MacGowan, F. Oshita, and Y. Ryu for measurement support; P. Huang and D. Tait for HEMT modeling; W. Bartoleme for layout support, and V. Zamora for MMIC fabrication.

References

[1] A. P. Chang, K. B. Niclas, B. D. Cantos, and W. A. Strifler, "Design and performance of a 2–18-GHz monolithic matrix amplifier," *IEEE Microwave and Millimeter-Wave Monolithic Circuit Symp. Dig.*, 1989, pp. 143–147.

[2] S. L. G. Chu, Y. Tajima, J. B. Cole, A. Platzker, and M. J. Schindler, "A novel 4–18-GHz monolithic matrix distributed amplifier," *IEEE Microwave and Millimeter-Wave Monolithic Circuit Symp. Dig.*, 1989, pp. 139–141.

[3] K. W. Kobayashi, R. Esfandiari, M. E. Hafizi, D. C. Streit, A. K. Oki, L. T. Tran, D. K. Umemoto, M. E. Kim, "GaAs HBT wideband matrix distributed and Darlington feedback amplifiers to 24 GHz," *IEEE Trans. Microwave Theory Tech.*, vol. 39, pp. 2001–2009, Dec. 1991.

[4] K. W. Chang, B. L. Nelson, A. K. Oki, and D. K. Umemoto, "2–19-GHz low power and high-IP3 monolithic HBT matrix amplifier," *IEEE Microwave Guided Wave Lett.*, vol. 2, pp. 17–19, Jan. 1992.